Interleukin-6 Inhibits Receptor Activator of Nuclear Factor κB Ligand-Induced Osteoclastogenesis by Diverting Cells into the Macrophage Lineage: Key Role of Serine[727] Phosphorylation of Signal Transducer and Activator of Transcription 3

Laurence Duplomb,* Marc Baud'huin,* Céline Charrier, Martine Berreur, Valérie Trichet, Frédéric Blanchard, and Dominique Heymann

Institut National de la Santé et de la Recherche Médicale (L.D., M.Ba., C.C., M.Be., V.T., F.B., D.H.), ERI 7, and Université de Nantes (L.D., M.Ba., C.C., M.Be., V.T., F.B., D.H.), Nantes atlantique universités, Laboratoire de Physiopathologie de la Résorption Osseuse et Thérapie des Tumeurs Osseuses Primitives, EA3822, Nantes F-44035, France; and Centre Hospitalier Universitaire (D.H.), Hôtel Dieu, Nantes 86021, France

Osteoclasts are bone-resorptive cells that differentiate from hematopoietic precursors upon receptor activator of nuclear factor κB ligand (RANKL) activation. Previous studies demonstrated that IL-6 indirectly stimulates osteoclastogenesis through the production of RANKL by osteoblasts. However, few data described the direct effect of IL-6 on osteoclasts. To investigate this effect, we used several models: murine RAW264.7 cells, mouse bone marrow, and human blood monocytes. In the three models used, the addition of IL-6 inhibited RANKL-induced osteoclastogenesis. Furthermore, IL-6 decreased the expression of osteoclast markers and up-modulated macrophage markers. To elucidate this inhibition, signal transducer and activator of transcription (STAT) 3, the main signaling molecule activated by IL-6, was analyzed. Ad-dition of two STAT3 inhibitors completely abolished RANKL-induced osteoclastogenesis, revealing a key role of STAT3. We demonstrated that a basal level of phosphorylated-STAT3 on Serine[727] associated with an absence of phosphorylation on Tyrosine[705] is essential for osteoclastogenesis. Furthermore, a decrease of Serine[727] phosphorylation led to an inhibition of osteoclast differentiation, whereas an increase of Tyrosine[705] phosphorylation upon IL-6 stimulation led to the formation of macrophages instead of osteoclasts. In conclusion, we showed for the first time that IL-6 inhibits RANKL-induced osteoclastogenesis by diverting cells into the macrophage lineage, and demonstrated the functional role of activated-STAT3 and its form of phosphorylation in the control of osteoclastogenesis. (*Endocrinology* 149: 3688–3697, 2008)

BONE REMODELING depends on osteoblast and osteoclast cells. Osteoblasts are responsible for bone apposition, whereas osteoclasts are specialized in bone resorption. Osteoclasts are multinucleated cells that differentiate from hematopoietic precursors localized in bone marrow and are closely related to macrophages (1, 2). Osteoclastic precursors differentiate into mature osteoclasts thanks to a tight interaction with osteoblastic/stromal cells: cell to cell interactions are necessary as well as the production of factors by osteoblasts (3–6). The receptor activator of nuclear factor κB ligand (RANKL), also called osteoprotegerin ligand, TNF-related activation-induced cytokine, or differentiation factor, is a key factor during osteoclastogenesis (7–12). RANKL

binds to its receptor, receptor activator of nuclear factor κB (RANK) present at the cell surface of osteoclast precursors and consequently activates different signal transduction pathways, leading to the formation and maturation of osteoclasts (13, 14). The binding of RANKL to RANK activates TNF receptor-associated factor adaptor proteins, particularly TNF receptor-associated factor 6, which in turn targets different proteins such as MAPKs, including ERK, p38, and c-Jun N-terminal kinase, and transcription factors such as nuclear factor-κB (NF-κB) or nuclear factor of activated T cells (6, 13, 15, 16). The phosphatidylinositol 3-kinase is also involved in osteoclastogenesis (17) as well as in the function of bone resorption of mature osteoclasts (18, 19).

IL-6 belongs to the gp130 family, which is composed of IL-6, IL-11, oncostatin M, leukemia inhibitory factor, cardiotrophin-1, and novel neurotrophin-1/B-cell stimulatory factor-3 (20, 21). They are pleiotropic cytokines, sharing the glycoprotein chain gp130 as a common signal transducer (20, 22, 23). The binding of IL-6 to its receptor leads to the activation of two main signal transduction pathways: the Janus kinase/signal transducer and activator of transcription (STAT) and the MAPK pathways. Activation of phosphatidylinositol 3-kinase after IL-6 stimulation has also been demonstrated in multiple myeloma cells for example (24). In

pathologies associated with bone loss, such as postmenopausal osteoporosis (25, 26), Paget's disease (27), multiple myeloma (28), rheumatoid arthritis (29), and hyperparathyroidism (30), elevation of IL-6 expression and secretion has been demonstrated (31). In bone microenvironment, IL-6 produced by stromal cells and osteoblasts but not by osteoclasts (32) has stimulated osteoclastogenesis. Indeed, IL-6 in association with its soluble receptor (soluble receptor IL-6) has been a good stimulator of bone resorption in a model of neonatal mouse calvaria (33) or in a model of mouse bone marrow cells in coculture with osteoblastic or stromal cells (34). However, this activity appears mainly due to the production of RANKL by osteoblastic cells, which in turn stimulates the differentiation of osteoclast precursors into osteoclasts, and, thus, induces their maturation and functions (33). Therefore, the effect of IL-6 on osteoclastogenesis can be defined as indirect through the production of RANKL by osteoblasts. However, the direct effect of IL-6 on osteoclastogenesis has never been described. The present study provides strong evidence that IL-6 directly inhibits RANKL-induced osteoclastogenesis in three models using only preosteoclastic cells in the absence of osteoblastic or stromal cells: the murine cell line RAW 264.7, mouse bone marrow cells, and human CD14$^+$ monocytes isolated from peripheral blood. Furthermore, we demonstrate the implication of STAT3 and its various phosphorylation forms during osteoclastogenesis.

Materials and Methods

Cell culture and osteoclast differentiation assays

Murine RAW 264.7 monocytic cells (American Type Culture Collection, Promochem, Molsheim, France) were cultured in phenol red-free α-MEM (Invitrogen, Eragny, France) supplemented with 10% fetal calf serum (FCS) (Perbio, Logan, UT), and 1% nonessential amino acids (Invitrogen). To induce osteoclast formation, RAW 264.7 cells were scraped and put back at 37 C for 2 min to allow adherence of the more differentiated cells. Nonadherent cells were then seeded in fresh medium at 3×10^3 or 10×10^3 cells in 96- or 24-well plates. After 2 h, recombinant human RANKL, kindly provided by Amgen Inc. (Thousand Oaks, CA), and recombinant human IL (hIL)-6 (R&D Systems, Abington, UK) were added at the concentration of 100 ng/ml (otherwise as noted in the figure legends). In some experiments, specific inhibitors of STAT3 (AG490 and STAT3 inhibitor peptide) or of the MAPK ERK1/2 (UO126) (Calbiochem, Fontenay sous Bois, France) were added at 5 and 100 μM, respectively. In some experiments, RAW 264.7 cells were pretreated with 100 ng/ml hIL-6 before induction of osteoclast differentiation. Multinucleated cells were counted under a light microscope [Leica DM IRB (Leica Microsystems GmbH, Wetzlar, Germany), Olympus D70 camera (Hamburg, Germany), and Olympus DP controller/manager analysis software] after May Grünwald/Giemsa (MGG) staining (Sigma, Saint Quentin-Fallavier, France) or tartrate-resistant acid phosphatase (TRAP) staining (Leukocyte Acid Phosphatase Assay kit; Sigma). All experiments were performed in triplicate at least three times.

Differentiation of mouse bone marrow cells into osteoclasts

Bone marrow cells were obtained by flushing femur and tibiae from 4-wk-old C57BL6 male mice. Total bone marrow cells were seeded in a 150-mm culture-treated petri dish in α-MEM containing 10% fetal calf serum and 1% penicillin/streptomycin. After 2 h, nonadherent cells were transferred in a new 150-mm petri dish for 18 h. After this second adherence, nonadherent cells were transferred in a nontreated petri dish in α-MEM containing 10% fetal calf serum, 1% penicillin/streptomycin, and 30 ng/ml mouse macrophage colony-stimulating factor (M-CSF). After 3 d, cells were detached by trypsin-EDTA treatment for 10 min, and then seeded at 350×10^3 cells per well in 24-well plates in the presence

of 10 ng/ml mouse M-CSF, with or without 100 ng/ml human RANKL (hRANKL) and 100 ng/ml hIL-6. Medium was changed every 4 d. TRAP staining was performed after 20-d culture. All experiments were performed in triplicate at least three times.

Differentiation of human CD14$^+$ cells into osteoclasts

Human peripheral blood mononuclear cells were isolated by centrifugation over Ficoll gradient (Sigma Chemicals Co., St. Louis, MO). CD14$^+$ cells were magnetically labeled with CD14 Microbeads and positively selected by MACS technology (Miltenyi Biotec, Bergisch Gladbach, Germany). CD14$^+$ cells were seeded in 24-well plates (250 $\times$ 10^3 cells per well) in α-MEM containing 10% FCS and 25 ng/ml human M-CSF. After 3-d culture, medium was changed with fresh medium containing 10% FCS, 25 ng/ml human M-CSF, with or without 100 ng/ml hRANKL, and with or without 100 ng/ml hIL-6. Thereafter, medium was changed every 4 d. The formation of osteoclasts occurred around 12-d culture and was observed by TRAP staining.

RNA isolation and real-time PCR

Total RNA was extracted using TRIzoL reagent (Invitrogen). First-strand cDNA was synthesized at 37 C for 1 h from 5 μg total RNA in a 50 μl mixture containing RT buffer, 0.5 μg Random Primers, 0.5 mM deoxynucleotide triphosphate mix, 20 U Rnasout, and 400 U Moloney murine leukemia virus-reverse transcriptase (all from Invitrogen). Sequences of primers used for real-time PCR are listed in Table 1. The real-time PCR contained, in a final volume of 10 μl, 10 ng reverse-transcribed total RNA, 300 nM of the forward and reverse primers, and 5 μl 2$\times$ SYBR green buffer (Bio-Rad, Marnes-la-Coquette, France). PCRs were performed in triplicate in 96-well plates, using the Chromo4 System (Bio-Rad). *Mus musculus* hypoxanthine guanine phosphoribosyl transferase 1 and cytochrome c-1 were used as an invariant control. Analysis was performed using the Vandesompele method (35).

Western blot analysis

RAW 264.7 and CD14$^+$ cells were cultured in the presence or not of 100 μM AG490 for 4 h at 37 C, and then stimulated with 25 ng/ml hIL-6 for 15 min. Extractions of cytoplasmic and nuclear proteins were performed with the NE-PER nuclear and cytoplasmic extraction kit from Pierce (Rockford, IL) according to the manufacturer's instructions. Protein concentrations were determined with the BCA protein assay (Sigma). Proteins were run on 10% SDS-PAGE and transferred to Immobilon-P membrane (Millipore, Bedford, MA). The membrane was blotted with antibodies to actin, phospho-STAT3 Tyr^{705} and phospho-STAT3 Ser^{727} (Cell Signaling Technologies, Beverly, MA), in PBS, 0.05% Tween 20, 3% BSA, washed, and probed with the secondary antibody coupled to horseradish peroxidase. The labeled proteins were detected using ECL reagent (Roche, Mannheim, Germany) according to the manufacturer's recommendations. Bands on Western blots were visualized using a CCD camera (Syngene G-Box; Syngene, Cambridge, UK), and

TABLE 1. Oligonucleotide primers used for real-time PCR

Gene	Accession no.	Primers sequence (5′–3′)
Hprt	NM_013556.2	TCCTCCTCAGACCGCTTTT
		CCTGGTTCATCATCGCTAATC
Cyc1	NM_025567.1	TGTGCTACACGGAGGAAGAA
		CATCATCATTAGGGCCATCC
TRAP (Acp5)	NM_007388	CGTCTCTGCACAGATTGCAT
		AAGCGCAAACGGTAGTAAGG
CTR	NM_007588	GAAGATGAGGTTCCTTCTCGTG
		GATCAAGGCCGGAGTCAGTG
Ctsk	NM_007802.2	GGAGGCGGCTATATGACCA
		GGCGTTATACATACAACTTTCATCC
RANK	NM_057149.1	AGACACAGAACGACTACCTGACTC
		GGCCCCACAATGTGTTGTA
Emr1	NM_010130	TCCTCCTTGCCTGGACACT
		GCCTTGAAGGTCAGCAACC
CD11b	NM_008401	GGCACGCAGACAGGAAGT
		CCCAGCAAGGGACCATTA

quantification of band densities was obtained using the Syngene Gene-Tool software. Experiments were performed four times for RAW 264.7 cells and twice for CD14$^+$ cells.

Luciferase activity

RAW 264.7 cells were cotransfected using lipofectamine 2000 reagent (Invitrogen) with pSiemLuc vectors expressing a Firefly luciferase reporter gene containing three copies of a STAT3 consensus binding site linked to a minimal thymidine kinase promoter (kindly provided by Dr. H. Gascan, Institut National de la Santé et de la Recherche Médicale Unité Mixte de Recherche 564, Angers, France) (36) and pRL-CMV as an internal control of transfection. pSiemLuc is a plasmid demonstrating STAT3 activity, and pZTK plasmid is the corresponding empty control vector. Luciferase activity was determined using the Dual Luciferase Reporter Assay system kit from Promega (Charbonnières, France) according to the manufacturer's recommendations. Experiments were performed three times.

Flow cytometry

At the end of the differentiation culture, RAW 264.7 cells were harvested with 0.02% EDTA, incubated with mouse seroblock to eliminate nonspecific binding, then incubated at 4 C for 30 min with different antibodies against macrophage specific markers [PE-CD11b (Mac-1), PE-F4/80, and mouse seroblock all from Serotec Ltd., Oxford, UK] in PBS containing 1% BSA, and then washed and fixed in PBS 1% formaldehyde. Irrelevant isotype-matched antibodies were used to determine levels of nonspecific binding. Flow cytometry analysis was performed on a FACScan using CELLQuest software (both from BD, Franklin Lakes, NJ). The experiment was performed at least three times.

Statistical analysis

The mean ± sd was calculated for all conditions and compared by ANOVA, with the Bonferroni multiple comparisons test as a *post hoc* test. Differences relative to a probability of two-tailed $P < 0.05$ were considered significant.

Results

IL-6 inhibits osteoclastogenesis on RAW 264.7 cells

To investigate the direct role of IL-6 on osteoclast differentiation, we examined the effect of IL-6 on RANKL-induced osteoclast formation from murine RAW 264.7 cells. RAW 264.7 cells were cultured for 5 d in the presence of 100 ng/ml hRANKL with or without 100 ng/ml hIL-6. After 4-d culture in the presence of hRANKL, a large number of multinucleated osteoclast-like cells (more than three nuclei) can be observed (Fig. 1A). Interestingly, although IL-6 alone had no effect on osteoclast differentiation of RAW 264.7 cells, 100 ng/ml hIL-6 added during the culture strongly inhibited the hRANKL-dependent osteoclast formation, and only a few and very small multinucleated cells persisted. Thus, the addition of IL-6 inhibited RANKL-induced osteoclast differentiation of RAW 264.7 cells in a dose-dependent manner (no inhibition at 1 ng/ml, 38% inhibition at 10 ng/ml and 81% inhibition at 100 ng/ml compared with the control without cytokine, $P < 0.05$) (Fig. 1B). Furthermore, IL-6 acted during the earliest steps of osteoclastic differentiation. Indeed, when IL-6 was added at d 1 of the experiment, RANKL-induced osteoclastogenesis was totally abolished, but if IL-6 was added at d 2 or 3, IL-6 had no effect on RANKL-induced osteoclastogenesis (Fig. 2A). To determine whether the inhibition of osteoclastogenesis induced by IL-6 was reversible or not, RAW 264.7 cells were cultured during 3 d with or without 100 ng/ml hIL-6 before adding hRANKL for 5 d with
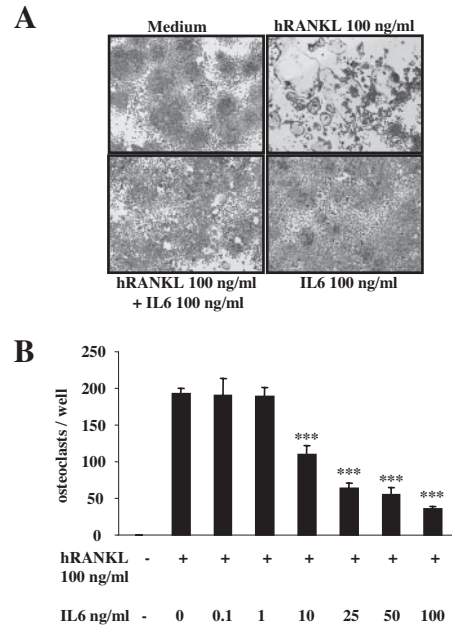

Fig. 1. IL-6 inhibits RANKL-induced osteoclastogenesis on RAW 264.7 cells. A, MGG staining of RAW 264.7 cells. RAW 264.7 cells were cultured for 5 d in the presence or not of 100 ng/ml hRANKL with or without 100 ng/ml hIL-6 (original magnification, ×100). B, Dose response of hIL-6 activity (0–100 ng/ml) in the presence of 100 ng/ml hRANKL to induce osteoclastogenesis. RAW 264.7 cells were stained with MGG, and multinucleated cells (more than three nuclei) were counted under a light microscope. Results are expressed as the number of multinucleated cells per well. Each value represents the mean (±sd) of multinucleated cells per well of a triplicate. All experiments were performed independently three times in triplicate. ***, $P < 0.001$ compared with hRANKL conditions.

or without hIL-6. As shown in Fig. 2B, the effect induced by hIL-6 was irreversible. Indeed, after being exposed for 3 d to hIL-6, RAW 264.7 cells were unable to differentiate into osteoclasts upon hRANKL activation. Interestingly, a new cell morphology appeared when RAW 264.7 cells were cultured for 5 d with hIL-6, and this became evident after 3 more days of culture (Fig. 2B). Indeed, the new large cells (*black arrows*) are characterized by a dense central zone containing nucleus and a poorly stained peripheral cytoplasm possessing numerous vacuoles. These cells also possessed numerous fine and dense filopodia. The cytological aspect of these cells is totally different from the multinucleated osteoclasts, and their size is smaller than osteoclasts. Thus, we hypothesized that these cells are macrophages, and we investigated this possibility.

IL-6 differentially modulates osteoclast and macrophage markers on RAW 264.7 cells

We next investigated the mRNA expression profile of some osteoclast and macrophage markers in RAW 264.7 cells cultured in the presence of 100 ng/ml hRANKL with or without 100 ng/ml hIL-6. Four specific osteoclast markers [TRAP, RANK, calcitonin receptor (CTR), and cathepsin K (Ctsk)] and two macrophage markers (Emr1 and CD11b) were analyzed by real-time PCR (Fig. 3A). As expected, hRANKL significantly increased osteoclastic markers: 11 times for TRAP, 24 times for CTR, and seven times for Ctsk.

A

FIG. 2. IL-6 acts during the earliest stages of differentiation, and its effect is irreversible. A, hIL-6 (100 ng/ml) was added to the hRANKL (100 ng/ml)-containing culture medium at d 1, 2, or 3 of the experiment. At d 5 of the culture, MGG staining was performed, and multinucleated cells (more than three nuclei) were counted under a light microscope. Results are expressed as the number of multinucleated cells per well. Each value represents the mean (±SD) of multinucleated cells per well of a triplicate experiment. The experiment was performed independently at least three times in triplicate. B, RAW 264.7 cells were pretreated with or without hIL-6 (100 ng/ml) for 3 d. Thereafter, cells were scrapped and put back in culture with the usual protocol of differentiation [*i.e.* 5 d in the presence or not of hRANKL (100 ng/ml) ± hIL6 (100 ng/ml)]. Cells were then stained with MGG. In the presence of IL-6, new cell morphologies appeared and are shown with *black arrows*. The experiment was performed at least four times in triplicate (original magnifications, ×100 and ×200). ***, $P < 0.001$.

B
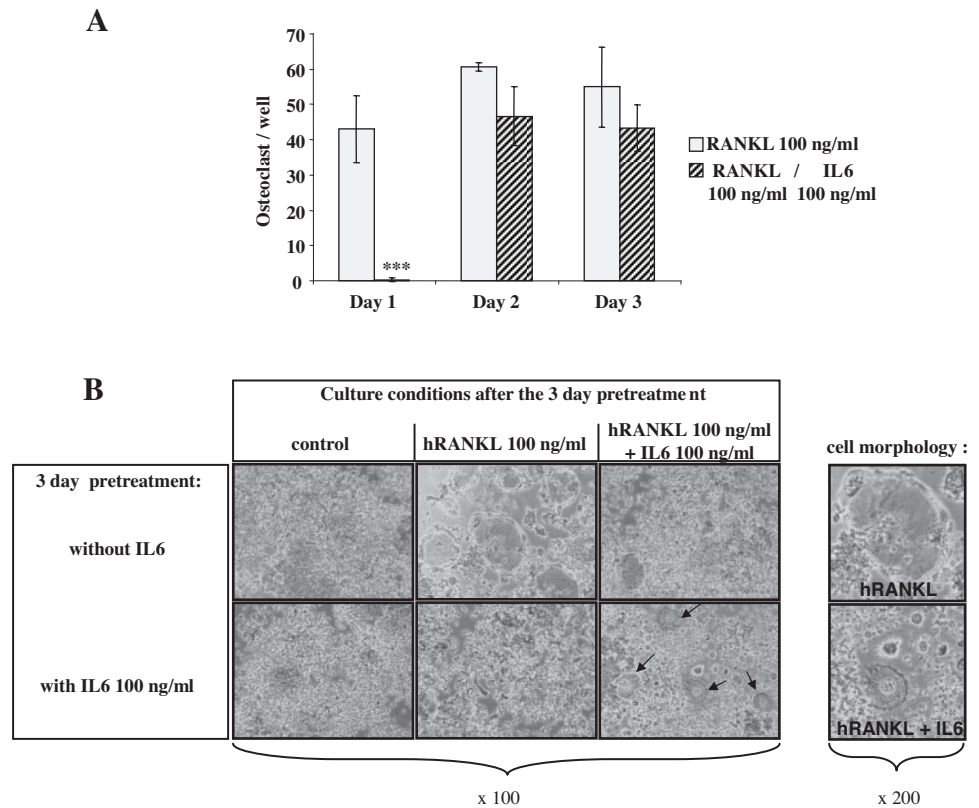
Moreover, the results clearly showed that hIL-6, even in the presence of hRANKL, strongly abolished the mRNA expression of the four osteoclastic markers studied. We next evaluated the mRNA expression of macrophagic markers such as CD11b and Emr1. RAW 264.7 cells expressed a basal level of these two markers, which were decreased during hRANKL-induced osteoclast differentiation. When hIL-6 was present in the culture medium, the mRNA expression of both macrophagic markers increased, even in the presence of hRANKL, confirming the hypothesis that hIL-6 induced a macrophage phenotype instead of an osteoclastic one.

Flow cytometry analysis was performed to confirm the phenotype of the RAW 264.7 cells cultured in the presence of hIL-6 and/or hRANKL (Fig. 3B). First experiments showed, after treatment with hIL-6, a very strong nonspecific background with the IgG2-PE isotype control. We observed that this high background was due to the presence of Fc-receptors CD16:CD32, induced at the RAW 264.7 cell surface by hIL-6 (data not shown). High expression of Fc-receptors is well known on macrophages, which is thus a first argument in favor of a macrophage differentiation induced by IL-6. To abolish the background as-

A

FIG. 3. IL-6 diverts RAW 264.7 cells into macrophages. A, RAW 264.7 cells were cultured in the presence or not of 100 ng/ml hRANKL with or without 100 ng/ml hIL-6. After 5 d in culture, mRNA expression of osteoclastic and macrophagic markers was analyzed by real-time PCR. Results are expressed as fold increase compared with the control. B, RAW 264.7 cells were cultured for 5 or 11 d in the presence or not of 100 ng/ml hRANKL with or without 100 ng/ml hIL-6. Cells were then analyzed for their expression of macrophagic markers by flow cytometry (faint curve = control unstimulated cells; *bold curve* = stimulated cells). Experiments were performed at least three times in triplicate. FL2-H, Fluorescence-2 height.

B
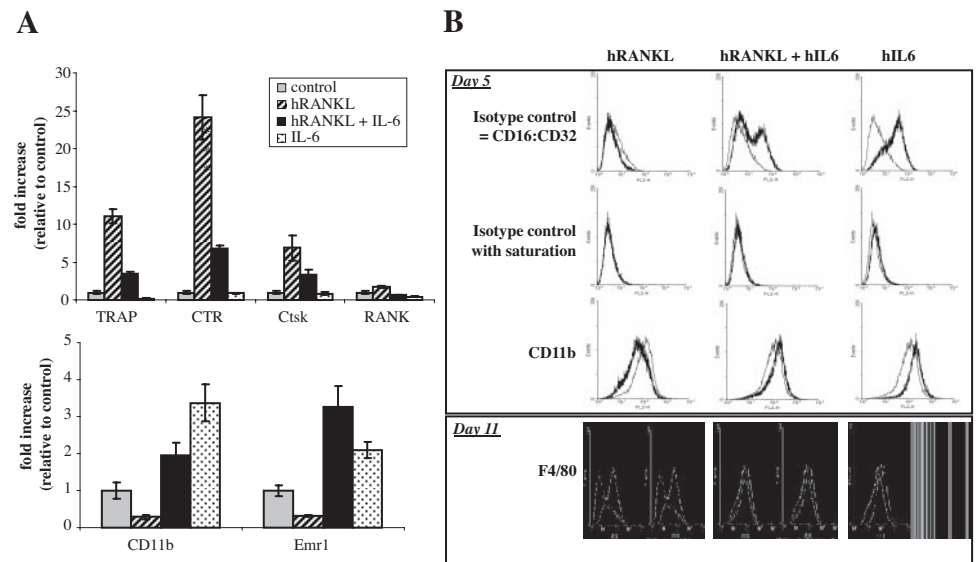
sociated with Fc-receptor expression, next experiments were performed with mouse seroblock reagent (anti-CD16:CD32 antibody) before incubation with specific antibodies. As shown in Fig. 3B, after 5-d culture, CD11b was increased with hIL-6 (with or without hRANKL), confirming our hypothesis. Because no significant effect was observed on F4/80 antigen (encoded by Emr1) after 5 d, we continued the culture of RAW 264.7 cells for 6 more days. At the end of this longer culture period, F4/80 expression was significantly increased at the cell surface of RAW 264.7 cells cultured in the presence of hIL-6 (with or without hRANKL). On the contrary, RANKL strongly down modulated F4/80 expression. Furthermore, TRAP staining performed at the end of these 11-d cultures showed that these cells remained in a TRAP negative state (data not shown). The up-regulation of CD16:CD32 and CD11b, and a bit later of F4/80 by hIL-6 confirmed the commitment of RAW 264.7 cells into the macrophage lineage. These results demonstrated that the inhibitory effect of hIL-6 on RANKL-induced osteoclastogenesis was due to the differentiation of RAW 264.7 into macrophages and not to a blockade into osteoclast precursors.

Recently, it has been shown that MafB, a protein of the Maf family selectively expressed in monocytes and macrophages, negatively regulates RANKL-induced osteoclastogenesis by down-regulation of nuclear factor of activated T-cell c1 and osteoclast-associated receptor, and induces macrophage differentiation (37). Thus, we hypothesized that IL-6 could up-regulate MafB in RAW 264.7 cells and then could divert cells to the macrophage lineage instead of the osteoclast one. However, no modulation of MafB was detected in our study (data not shown).

Serine[727]-phosphorylated STAT3 is mandatory for osteoclastogenesis

To understand further the mechanism of action of hIL-6, we focused our investigations on the STAT-3 transcription factor and MAPK, the two main signal transduction pathways induced by IL-6. UO126, a specific inhibitor of MAPK ERK1/2, did not reverse the inhibitory effect of IL-6 on hRANKL-induced osteoclastogenesis, but, as previously shown by Hotokezaka *et al.* (38), UO126 significantly increased RANKL-induced osteoclastogenesis (data not shown). Two specific inhibitors of STAT3, AG490 and a STAT3-inhibitor peptide, were used to determine the involvement of the STAT3 signaling pathway in the IL-6 effects on osteoclastogenesis. At the concentrations used, cells grew normally, and no toxicity was observed with these inhibitors (data not shown). As shown in Fig. 4, A and B, STAT3 inhibitors did not reverse the inhibitory effect of hIL6 on hRANKL-induced osteoclastogenesis of RAW 264.7 cells. However, an unexpected result showed that in the presence of hRANKL and STAT3 inhibitors, the osteoclastogenesis was completely blocked, indicating for the first time the essential role played by STAT3 during osteoclastogenesis induced by RANKL. Because STAT3 is not activated by hRANKL (data not shown), the constitutively activated phosphorylated forms of STAT3 were analyzed by Western blots. Even if nuclear import is independent of phosphorylation, Tyrosine[705] phosphorylation is necessary for STAT3 activation, inducing STAT3 to dimerize, translocate to the nucleus, bind to DNA, and induce specific gene transcription (39, 40). Constitutive phosphorylation of Tyrosine[705] STAT3 was not detected in RAW 264.7 cells in cytoplasmic or nuclear fractions, but as expected, hIL-6 treatment of RAW 264.7

FIG. 4. STAT3 and its phosphorylation tightly control osteoclastogenesis. RAW 264.7 cells were cultured in the presence of two STAT3 inhibitors, AG490 (5 μM) (A) and STAT 3 inhibitor peptide (100 μM) (B), with or without 100 ng/ml hRANKL and with or without 25 ng/ml hIL-6. After 5-d culture, MGG staining was performed, and multinucleated cells (more than three nuclei) were counted under a light microscope. C, RAW 264.7 cells were cultured for 4 h in the presence or not of 100 μM AG490 and then stimulated or not with IL-6 for 15 min. Western blot analysis was performed on cell lysate to determine the level of STAT3 phosphorylated on Tyrosine[705] or Serine[727]. Actin informed about equal loading charge. Below the Western blot, *histograms* showed the band intensities quantified using GeneTool software and represented as a ratio to actin signals. Experiments were performed four times. D, Luciferase activity in RAW 264.7 cells was measured 48 h after transfection with pSiemLuc, which is a plasmid demonstrating STAT3 activity, or its corresponding control empty vector (pZTK plasmid). Ct, Control medium.
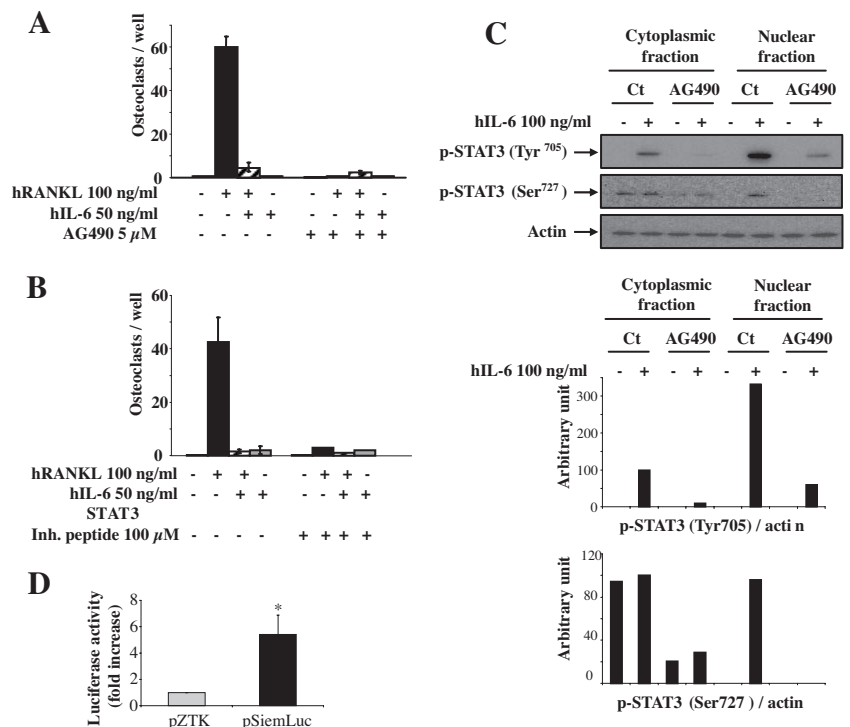
cells for 15 min induced a strong activation of phospho-Tyrosine[705] STAT3 in both cytoplasmic and nuclear fractions (Fig. 4C). In contrast, phospho-Serine[727] was detected at a basal level in unstimulated cells, and the up-regulation after IL-6 treatment was mainly observed in the nuclear fraction of these cells. Furthermore, we estimated the level of endogenous active STAT3 using a luciferase reporter gene containing three copies of a STAT3 consensus binding site linked to a minimal thymidine kinase promoter. In these conditions, luciferase activity correlated with active STAT3. As shown in Fig. 4C, RAW 264.7 cells expressed a basal level of endogenous active STAT3. Although this experiment could not reveal which form of STAT3 was active, it evidenced that this activity was associated with phospho-Serine[727] STAT3. The addition of 100 μM AG490 for 4 h inhibited the IL-6 induced STAT3-Tyrosine[705] and Serine[727] phosphorylations, as well as the basal level of phospho-Serine[727] in the control condition without hIL-6 (Fig. 4C). These observations evidenced that a sufficient level of constitutive activation of STAT3 by phosphorylation on Serine[727] is mandatory to generate osteoclasts because the presence of AG490 inhibited osteoclastogenesis (Fig. 4A) by reducing the level of Serine[727] phosphorylated STAT3 (Fig. 4C).

Furthermore, we checked NF-κB signaling in cells pretreated with IL-6: cells were treated or not with hIL-6 for 3 d before hRANKL stimulation (100 ng/ml, 20 min). As expected, hRANKL induced the phosphorylation of p65 and p105 in control conditions. When hIL-6 was present for 3 d before hRANKL stimulation, the induction of phosphorylation of p105 and p65 still remained, with the same intensity observed upon hRANKL stimulation. Therefore, hIL-6 does not modulate hRANKL induced-NF-κB signaling (data not shown).

IL-6 inhibits RANKL-induced osteoclastogenesis of mouse bone marrow cells and human CD14$^+$ monocytes

To confirm the inhibitory effect of IL-6 on osteoclastogenesis, similar experiments were performed using two other models of osteoclast generation: mouse bone marrow cells and human CD14$^+$ monocytes isolated from peripheral blood cultured in the presence of M-CSF and RANKL. Indeed, after 20 d, 234 ± 59 TRAP-positive multinucleated cells were generated from mouse bone marrow cells cultured in the presence of M-CSF and hRANKL, whereas only 40 ± 8 TRAP-positive multinucleated cells were formed in the presence of hIL-6 (Fig. 5). This result is in agreement with the results obtained on the RAW 264.7 cell model and confirms the inhibitory effect of hIL6 on RANKL-induced osteoclastogenesis. Similar results were obtained using purified human CD14$^+$ monocytes (Fig. 6). Indeed, in the presence of hRANKL, 275 ± 20 osteoclasts were counted, whereas the number of TRAP positive multinucleated cells was reduced by 87% in the presence of hIL-6 (Fig. 6, A and B). The involvement of Serine[727]-phosphorylated STAT3 in osteoclastogenesis was confirmed in these models. Indeed, in control condition, a basal level of STAT3 phosphorylated on Serine[727] can be observed in human CD14$^+$ monocytes, whereas no phosphorylation on Tyrosine[705] was detected. IL-6 stimulated both Serine[727] and Tyrosine[705] phosphory-
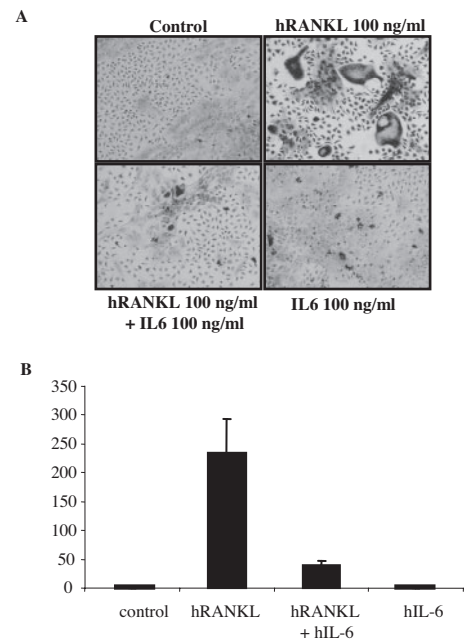

FIG. 5. IL-6 inhibits hRANKL-induced osteoclastogenesis from mouse bone marrow cells. Mouse bone marrow cells were cultured for 20 d in the presence or the absence of 100 ng/ml hRANKL with or without 100 ng/ml IL-6. TRAP staining was performed (A), and TRAP$^+$ multinucleated cells were counted (B) under a light microscope. Results are expressed as number of TRAP$^+$ multinucleated cells (more than three nuclei) per well. Each value represents the mean (±SD) of osteoclast per well of a triplicate experiment. Experiments were performed independently at least three times (original magnification, ×100).

lations, and this effect was decreased in the presence of AG490 (Fig. 6C).

Discussion

IL-6 is enhanced in pathological situations of bone loss, such as multiple myeloma (41), Paget's disease (27), periodontal disease (42), hyperparathyroidism (30), and rheumatoid arthritis (29). For this reason the role of IL-6 has often been studied *in vitro* using different models of coculture of osteoblast and osteoclast progenitors. These studies have reported a pro-osteoclastic activity of IL-6 (33, 34) with a direct effect of this cytokine on osteoblasts inducing the production of RANKL, which in turn activates the differentiation of osteoclast progenitors into osteoclasts. However, the influence of IL-6 on osteoclastogenesis remains disputed (43). Indeed, Kudo *et al.* (44) showed that IL-6 alone induced osteoclastogenesis from human CD14$^+$ monocytes in the absence of RANKL, results in favor of a pro-resorption activity of IL-6. Their results are in accordance with those of Gao *et al.* (45), who revealed the expression of IL-6 receptors on osteoclast progenitors and mature osteoclasts. Similarly, De Benedetti *et al.* (46) reported that IL-6 overexpression in prepubertal mice causes an increased osteoclastogenesis, leading to an accelerated bone resorption. On the contrary, Kitamura *et al.* (47) generated transgenic mice overexpressing hIL-6, which presented a decrease in osteoclast number and bone resorption measured by histomorphometry. The difference observed in these two studies had already been dis-

A

B

C

FIG. 6. IL-6 inhibits hRANKL-induced osteoclastogenesis from purified human CD14$^+$ cells. Purified human CD14+ monocytes isolated from peripheral blood were cultured for 12 d in the presence or not of 100 ng/ml hRANKL with or without 100 ng/ml IL-6. TRAP staining was then performed (A), and TRAP$^+$ multinucleated cells (more than three nuclei) were counted (B) under a light microscope (original magnification, ×100). Experiments were performed independently more than three times. C, Human CD14$^+$ monocytes were cultured 4 h in the presence or absence of 100 μM AG490 and then stimulated or not with 100 ng/ml hIL-6 for 15 min. Western blot analysis was performed on cell lysates to determine the level of phospho-Tyrosine^{705} and -Serine^{727} STAT3. Actin informed about equal loading charge. Below the Western blot, *histograms* showed the band intensities quantified using GeneTool software and represented as a ratio to actin signals. Experiments were performed three times independently. Ct, Control medium.
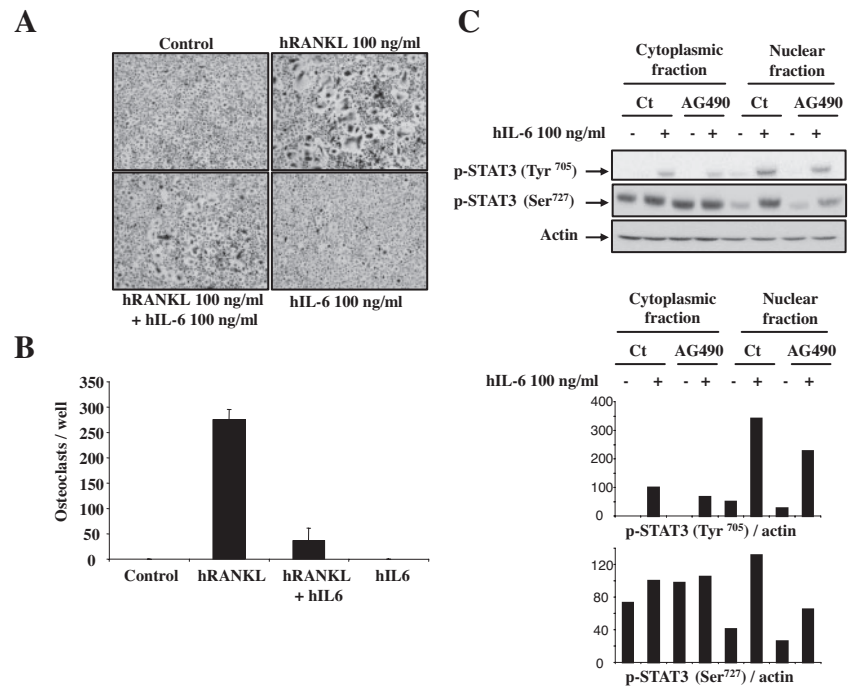
cussed by De Benedetti *et al.* (46), who suggested that the impact of IL-6 on osteoclasts may depend on the age of the animal. Indeed, De Benedetti *et al.* (46) studied prepubertal mice, whereas Kitamura *et al.* (47) studied adult mice. This phenomenon relative to the development of the animal had been observed by Hoshino *et al.* (48) in a model of collagen-induced arthritis in rats. Adult rats showed a decrease in bone resorption due to a decrease in osteoclastogenesis, whereas prepubertal rats displayed an increase of bone resorption and an increased number of osteoclasts. In the present study, we have explored the direct effect of IL-6 on osteoclast progenitors obtained from three different models (RAW 264.7 cell line, mouse bone marrow cells, and human CD14$^+$ monocytes), and demonstrated in these three models that IL-6 targeted osteoclast precursors and inhibited RANKL-induced osteoclastogenesis, diverting them into the macrophage lineage. Similarly, Flanagan *et al.* (49) demonstrated that IL-6 failed to induce bone resorption in contrast to vitamin D3. These apparent discrepancies could be explained by the model of osteoclastogenesis and especially the experimental conditions used (serum, medium, *etc.*), and by the potential interaction of IL-6 signaling with Ca^{2+} sensing (50). Indeed, Ca^{2+} levels strongly affect osteoclastogenesis, and modulate the expression of IL-6 and IL6 receptors. Such an autocrine-paracrine loop may affect osteoclastic activity in the face of Ca^{2+} level generated locally during resorption and present in the serum and culture medium. A dual function of IL-6 cannot be excluded depending on the biological microenvironment (ions, cytokines, *etc.*). IL-6 may be considered as a pro-resorption factor as well as a protector of bone. Indeed, high IL-6 concentration produced during osteolytic pathologies may reflect a protective mechanism of the skeleton to compensate increased bone resorption especially induced by RANKL. IL-6 may then be produced to counterbalance the high RANKL concentrations produced in bone

microenvironment. Such a protective mechanism has been envisaged for osteoprotegerin in osteoporosis (51).

The transcription factor STAT3 and the SHP2/ras/MAPK pathway are the two main signaling pathways activated by IL-6. Their implications during osteoclastogenesis have been proven directly in osteoclasts and indirectly through the production of RANKL by osteoblast cells. Indeed, STAT3 is activated in osteoblasts or stromal cells upon IL-6 stimulation, and it leads to the production of RANKL for induction of osteoclastogenesis (52). In osteoclasts, the role of STAT3 is controversial. Kim *et al.* (53) demonstrated that an inhibitor of STAT3 (PIAS3) completely abolished osteoclastogenesis, whereas other studies showed an increased number of osteoclasts generated from STAT3 deficient osteoclast precursors (54). Furthermore, Sims *et al.* (55) used knock-in gp130 mutant mice unable to elicit either gp130-dependent STAT1/3 or SHP2/ras/MAPK activation and suggested that MAPK activation in osteoclasts inhibits osteoclastogenesis, whereas STAT3 in osteoblasts increases osteoclastogenesis through the production of RANKL. Some recent studies indirectly demonstrated the importance of STAT3 in bone physiology. Indeed, STAT3 mutations in its DNA-binding domain cause hyper-IgE syndrome, which is associated with skeletal/dental abnormalities, bone fragility due to increased bone resorption and decreased mineralization (56–58).

In the present study, we confirm the inhibitory role of the MAPK ERK1/2 during hRANKL-induced osteoclastogenesis (38), but we did not confirm the implication of the gp130-SHP2/ras/MAPK pathway in the inhibitory role of IL-6 in osteoclast differentiation. In contrast, the key role of STAT3 and its various forms of phosphorylation were evidenced in osteoclast precursors. Indeed, inhibition of STAT3 by AG490 or STAT3 inhibitor peptide totally prevented hRANKL-induced osteoclastogenesis. Osteoclast precursors express a basal level of Serine^{727}-phosphorylated STAT3 at both cyto-

plasmic and nuclear localization, this form being active as revealed by luciferase assay. This result is in agreement with the work of Liu *et al.* (59), which demonstrated in a macrophage cell line a basal level of Serine[727] phosphorylation without any detection of Tyrosine[705] phosphorylation. Furthermore, we showed that Tyrosine[705] phosphorylation, which is undetectable at the basal level but enhanced after IL-6 stimulation, prevailed over the activation of Serine[727] phosphorylation, inducing differentiation of RAW 264.7 cells into macrophages and, thus, inhibiting RANKL-induced osteoclastogenesis. Thus, our study indicates that Tyrosine[705]-phosphorylated STAT3 is involved in the inhibition of osteoclastogenesis by IL-6, whereas a basal level of Serine[727]-phosphorylated STAT3 is mandatory to support osteoclastogenesis (Fig. 7).

The role of Serine[727] phosphorylation remains unclear. It is generally suggested that Serine[727] phosphorylation of STAT3, and even other STATs such as STAT1, is required to achieve a complete and maximal transcriptional activity of STATs (60, 61). However, some transcriptional activity of STAT3 only phosphorylated on Serine[727] has also been demonstrated (62, 63). Chung *et al.* (64) had suggested that phosphorylation of STAT3 on Tyrosine[705] or Serine[727] can be two independent phenomena, which can be induced and regulated independently. This group and others proposed an inhibitory effect of Serine[727] phosphorylation on Tyrosine[705] phosphorylation (64, 65). Thus, even if Tyrosine[705] phosphorylation of STAT3 has always been suggested as required for STAT3 activation, some studies agree to give more importance to Serine[727] phosphorylation. For example, Serine[727] phosphorylation mediates the expression of Mcl1 in macrophages (59) or induces transcriptional activity upon nerve growth factor stimulation on PC12 cells (66).

Interconnections between NF-κB, usually activated by the TNF superfamily cytokines, including RANKL, and STAT3 mostly activated by the gp130 cytokine family have been recently evidenced (67). These authors demonstrated the constitution of a novel transcription factor complex, formed by the unphosphorylated form of STAT3 bound to unphosphorylated NF-κB, a complex able to compete with inhibitor κB. The complex unphosphorylated STAT3-NF-kB accumulates in the nucleus and activates specific genes. Furthermore, they evidenced a feedback loop in which IL-6 induces the phosphorylation of STAT3 leading, in a second step, to an increase of unphosphorylated STAT3 interacting with NF-κB. A similar mechanism may be hypothesized to explain the cross talk between IL-6 and RANKL (68), especially the inhibitory effect of IL-6 on RANKL-induced osteoclastogenesis. In our present data, IL-6 inhibits RANKL-induced osteoclastogenesis, revealing a functional cross talk between IL-6 and RANKL.

In conclusion, the present work reveals a key role of STAT3 Serine[727] phosphorylation during osteoclastogenesis, and allows clarifying the balance between MAPK ERK1/2 and STAT3 in the bone biology. Thus, our data suggest a dual role of STAT3 depending on the cells (osteoblast or osteoclast) and its phosphorylation form. Indeed, STAT3 in osteoblasts is a pro-osteoclastic molecule inducing the production of RANKL (55). In osteoclasts, STAT3 phosphorylated on Serine[727] is also a pro-osteoclastic molecule, but as soon as STAT3 phosphorylated on Tyrosine[705] becomes in excess of STAT3 phosphorylated on Serine[727] (*e.g.* after IL-6 stimulation), STAT3 becomes an antiosteoclastic molecule. Here, we also evidenced a dual role of IL-6 depending on its target cell. On osteoblast, IL-6 is a pro-resorptive cytokine, whereas on osteoclast, IL-6 is an antiresorptive cytokine. Further investigations are needed to clarify the involvement of STAT3, NF-κB, and MAPK ERK1/2 interrelations in osteoclast differentiation to better define novel therapeutic strategies of osteolytic disorders. In pathologies associated with bone loss, such as postmenopausal osteoporosis, Paget's disease, multiple myeloma, rheumatoid arthritis, and hyperparathyroidism, elevation of IL-6 expression and secretion has been demonstrated, and clinical trials using neutralizing IL-6 an-

FIG. 7. Schematic representation of the implication of STAT3 during osteoclast or macrophage differentiation. In undifferentiated pre-osteoclast cells, a pool of Serine (Ser)[727]-phosphorylated STAT3 is present at a sufficient level and is mandatory for the formation of osteoclast upon RANKL stimulation. In the presence of AG490, Serine[727]-phosphorylated STAT3 is decreased and is not sufficient to support osteoclastogenesis, leading to the nondifferentiation of osteoclast progenitors. Upon IL-6 stimulation, both Serine[727] and Tyrosine (Tyr)[705] are phosphorylated, but Tyrosine[705] phosphorylation prevailed against Serine[727] phosphorylation and leads to inhibition of osteoclastogenesis and induction of macrophage differentiation.
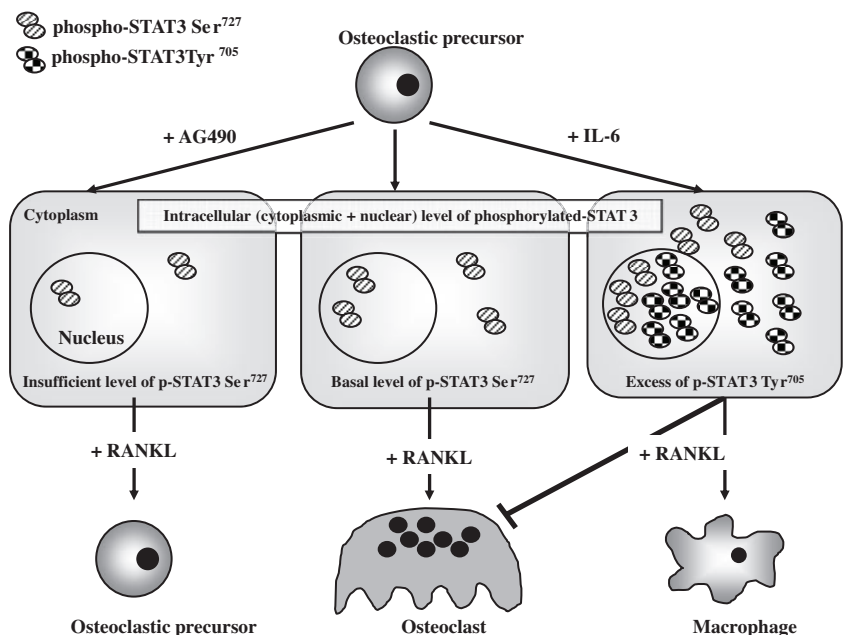
tibodies are in progress. In this context a better comprehension of IL-6 activities on bone cells and its molecular mode of action are necessary to develop new and more effective therapies. Our results suggest that better antiresorption treatments could be achieved by targeting more specifically the deleterious effects of IL-6 on osteoblasts and leaving the beneficial antiresorptive effects on osteoclasts. This could be obtained by a specific inhibition of STAT3 in osteoblast, and not in osteoclast.

Acknowledgments

References

1. **Chambers TJ** 2000 Regulation of the differentiation and function of osteoclasts. J Pathol 192:4–13
2. **Roodman GD** 2006 Regulation of osteoclast differentiation. Ann NY Acad Sci 1068:100–109
3. **Epker BN, Frost HM** 1965 Correlation of bone resorption and formation with the physical behavior of loaded bone. J Dent Res 44:33–41
4. **Ilvesaro J, Tuukkanen J** 2003 Gap-junctional regulation of osteoclast function. Crit Rev Eukaryot Gene Expr 13:133–146
5. **Heymann D, Guicheux J, Gouin F, Passuti N, Daculsi G** 1998 Cytokines, growth factors and osteoclasts. Cytokine 10:155–168
6. **Theoleyre S, Wittrant Y, Tat SK, Fortun Y, Redini F, Heymann D** 2004 The molecular triad OPG/RANK/RANKL: involvement in the orchestration of pathophysiological bone remodeling. Cytokine Growth Factor Rev 15:457–475
7. **Takahashi N, Udagawa N, Suda T** 1999 A new member of tumor necrosis factor ligand family, ODF/OPGL/TRANCE/RANKL, regulates osteoclast differentiation and function. Biochem Biophys Res Commun 256:449–455
8. **Yasuda H, Shima N, Nakagawa N, Yamaguchi K, Kinosaki M, Mochizuki S, Tomoyasu A, Yano K, Goto M, Murakami A, Tsuda E, Morinaga T, Higashio K, Udagawa N, Takahashi N, Suda T** 1998 Osteoclast differentiation factor is a ligand for osteoprotegerin/osteoclastogenesis-inhibitory factor and is identical to TRANCE/RANKL. Proc Natl Acad Sci USA 95:3597–3602
9. **Lacey DL, Timms E, Tan HL, Kelley MJ, Dunstan CR, Burgess T, Elliott R, Colombero A, Elliott G, Scully S, Hsu H, Sullivan J, Hawkins N, Davy E, Capparelli C, Eli A, Qian YX, Kaufman S, Sarosi I, Shalhoub V, Senaldi G, Guo J, Delaney J, Boyle WJ** 1998 Osteoprotegerin ligand is a cytokine that regulates osteoclast differentiation and activation. Cell 93:165–176
10. **Kong YY, Yoshida H, Sarosi I, Tan HL, Timms E, Capparelli C, Morony S, Oliveira-dos-Santos AJ, Van G, Itie A, Khoo W, Wakeham A, Dunstan CR, Lacey DL, Mak TW, Boyle WJ, Penninger JM** 1999 OPGL is a key regulator of osteoclastogenesis, lymphocyte development and lymph-node organogenesis. Nature 397:315–323
11. **Wong BR, Rho J, Arron J, Robinson E, Orlinick J, Chao M, Kalachikov S, Cayani E, Bartlett 3rd FS, Frankel WN, Lee SY, Choi Y** 1997 TRANCE is a novel ligand of the tumor necrosis factor receptor family that activates c-Jun N-terminal kinase in T cells. J Biol Chem 272:25190–25194
12. **Baud'huin M, Duplomb L, Ruiz Velasco C, Fortun Y, Heymann D, Padrines M** 2007 Key roles of the OPG-RANK-RANKL system in bone oncology. Expert Rev Anticancer Ther 7:221–232
13. **Boyle WJ, Simonet WS, Lacey DL** 2003 Osteoclast differentiation and activation. Nature 423:337–342
14. **Wittrant Y, Theoleyre S, Couillaud S, Dunstan C, Heymann D, Redini F** 2004 Relevance of an in vitro osteoclastogenesis system to study receptor activator of NF-kB ligand and osteoprotegerin biological activities. Exp Cell Res 293:292–301
15. **Blair HC, Robinson LJ, Zaidi M** 2005 Osteoclast signalling pathways. Biochem Biophys Res Commun 328:728–738
16. **Matsumoto M, Sudo T, Saito T, Osada H, Tsujimoto M** 2000 Involvement of p38 mitogen-activated protein kinase signaling pathway in osteoclastogenesis mediated by receptor activator of NF-κB ligand (RANKL). J Biol Chem 275:31155–31161
17. **Lee SE, Woo KM, Kim SY, Kim HM, Kwack K, Lee ZH, Kim HH** 2002 The phosphatidylinositol 3-kinase, p38, and extracellular signal-regulated kinase pathways are involved in osteoclast differentiation. Bone 30:71–77
18. **Hall TJ, Jeker H, Schaueblin M** 1995 Wortmannin, a potent inhibitor of phosphatidylinositol 3-kinase, inhibits osteoclastic bone resorption in vitro. Calcif Tissue Int 56:336–338
19. **Nakamura I, Takahashi N, Sasaki T, Tanaka S, Udagawa N, Murakami H, Kimura K, Kabuyama Y, Kurokawa T, Suda T, Fukui Y** 1995 Wortmannin, a specific inhibitor of phosphatidylinositol-3 kinase, blocks osteoclastic bone resorption. FEBS Lett 361:79–84
20. **Heinrich PC, Behrmann I, Muller-Newen G, Schaper F, Graeve L** 1998 Interleukin-6-type cytokine signalling through the gp130/Jak/STAT pathway. Biochem J 334(Pt 2):297–314
21. **Senaldi G, Varnum BC, Sarmiento U, Starnes C, Lile J, Scully S, Guo J, Elliott G, McNinch J, Shaklee CL, Freeman D, Manu F, Simonet WS, Boone T, Chang MS** 1999 Novel neurotrophin-1/B cell-stimulating factor-3: a cytokine of the IL-6 family. Proc Natl Acad Sci USA 96:11458–11463
22. **Heinrich PC, Behrmann I, Haan S, Hermanns HM, Muller-Newen G, Schaper F** 2003 Principles of interleukin (IL)-6-type cytokine signalling and its regulation. Biochem J 374(Pt 1):1–20
23. **Kishimoto T, Akira S, Narazaki M, Taga T** 1995 Interleukin-6 family of cytokines and gp130. Blood 86:1243–1254
24. **Hideshima T, Nakamura N, Chauhan D, Anderson KC** 2001 Biologic sequelae of interleukin-6 induced PI3-K/Akt signaling in multiple myeloma. Oncogene 20:5991–6000
25. **Manolagas SC, Jilka RL** 1995 Bone marrow, cytokines, and bone remodeling. Emerging insights into the pathophysiology of osteoporosis. N Engl J Med 332:305–311
26. **Girasole G, Jilka RL, Passeri G, Boswell S, Boder G, Williams DC, Manolagas SC** 1992 17β-Estradiol inhibits interleukin-6 production by bone marrow-derived stromal cells and osteoblasts in vitro: a potential mechanism for the antiosteoporotic effect of estrogens. J Clin Invest 89:883–891
27. **Roodman GD** 2001 Studies in Paget's disease and their relevance to oncology. Semin Oncol 28(Suppl 11):15–21
28. **Klein B, Zhang XG, Jourdan M, Boiron JM, Portier M, Lu ZY, Wijdenes J, Brochier J, Bataille R** 1990 Interleukin-6 is the central tumor growth factor in vitro and in vivo in multiple myeloma. Eur Cytokine Net 1:193–201
29. **Kotake S, Sato K, Kim KJ, Takahashi N, Udagawa N, Nakamura I, Yamaguchi A, Kishimoto T, Suda T, Kashiwazaki S** 1996 Interleukin-6 and soluble interleukin-6 receptors in the synovial fluids from rheumatoid arthritis patients are responsible for osteoclast-like cell formation. J Bone Miner Res 11:88–95
30. **Grey A, Mitnick MA, Shapses S, Ellison A, Gundberg C, Insogna K** 1996 Circulating levels of interleukin-6 and tumor necrosis factor-α are elevated in primary hyperparathyroidism and correlate with markers of bone resorption–a clinical research center study. J Clin Endocrinol Metab 81:3450–3454
31. **Heymann D, Rousselle AV** 2000 gp130 cytokine family and bone cells. Cytokine 12:1455–1468
32. **Holt I, Davie MW, Marshall MJ** 1996 Osteoclasts are not the major source of interleukin-6 in mouse parietal bones. Bone 18:221–226
33. **Palmqvist P, Persson E, Conaway HH, Lerner UH** 2002 IL-6, leukemia inhibitory factor, and oncostatin M stimulate bone resorption and regulate the expression of receptor activator of NF-κB ligand, osteoprotegerin, and receptor activator of NF-κB in mouse calvariae. J Immunol 169:3353–3362
34. **Tamura T, Udagawa N, Takahashi N, Miyaura C, Tanaka S, Yamada Y, Koishihara Y, Ohsugi Y, Kumaki K, Taga T, Kishimoto T, Suda T** 1993 Soluble interleukin-6 receptor triggers osteoclast formation by interleukin 6. Proc Natl Acad Sci USA 90:11924–11928
35. **Vandesompele J, De Preter K, Pattyn F, Poppe B, Van Roy N, De Paepe A, Speleman F** 2002 Accurate normalization of real-time quantitative RT-PCR data by geometric averaging of multiple internal control genes. Genome Biol 3:RESEARCH0034
36. **Coqueret O, Gascan H** 2000 Functional interaction of STAT3 transcription factor with the cell cycle inhibitor p21WAF1/CIP1/SDI1. J Biol Chem 275:18794–18800
37. **Kim K, Kim JH, Lee J, Jin HM, Kook H, Kim KK, Lee SY, Kim N** 2007 MafB negatively regulates RANKL-mediated osteoclast differentiation. Blood 109:3253–3259
38. **Hotokezaka H, Sakai E, Kanaoka K, Saito K, Matsuo K, Kitaura H, Yoshida N, Nakayama K** 2002 U0126 and PD98059, specific inhibitors of MEK, accelerate differentiation of RAW264.7 cells into osteoclast-like cells. J Biol Chem 277:47366–47372
39. **Reich NC, Liu L** 2006 Tracking STAT nuclear traffic. Nat Rev Immunol 6:602–612
40. **Darnell Jr JE** 1997 STATs and gene regulation. Science 277:1630–1635
41. **Klein B, Wijdenes J, Zhang XG, Jourdan M, Boiron JM, Brochier J, Liautard**

J, Merlin M, Clement C, Morel-Fournier B 1991 Murine anti-interleukin-6 monoclonal antibody therapy for a patient with plasma cell leukemia. Blood 78:1198–1204

42. **Loos BG, Craandijk J, Hoek FJ, Wertheim-van Dillen PM, van der Velden U** 2000 Elevation of systemic markers related to cardiovascular diseases in the peripheral blood of periodontitis patients. J Periodontol 71:1528–1534

43. **Rousselle AV, Heymann D** 2002 Osteoclastic acidification pathways during bone resorption. Bone 30:533–540

44. **Kudo O, Sabokbar A, Pocock A, Itonaga I, Fujikawa Y, Athanasou NA** 2003 Interleukin-6 and interleukin-11 support human osteoclast formation by a RANKL-independent mechanism. Bone 32:1–7

45. **Gao Y, Morita I, Maruo N, Kubota T, Murota S, Aso T** 1998 Expression of IL-6 receptor and GP130 in mouse bone marrow cells during osteoclast differentiation. Bone 22:487–493

46. **De Benedetti F, Rucci N, Del Fattore A, Peruzzi B, Paro R, Longo M, Vivarelli M, Muratori F, Berni S, Ballanti P, Ferrari S, Teti A** 2006 Impaired skeletal development in interleukin-6-transgenic mice: a model for the impact of chronic inflammation on the growing skeletal system. Arthritis Rheum 54:3551–3563

47. **Kitamura H, Kawata H, Takahashi F, Higuchi Y, Furuichi T, Ohkawa H** 1995 Bone marrow neutrophilia and suppressed bone turnover in human interleukin-6 transgenic mice. A cellular relationship among hematopoietic cells, osteoblasts, and osteoclasts mediated by stromal cells in bone marrow. Am J Pathol 147:1682–1692

48. **Hoshino K, Hanyu T, Arai K, Takahashi HE** 2001 Mineral density and histomorphometric assessment of bone changes in the proximal tibia early after induction of type II collagen-induced arthritis in growing and mature rats. J Bone Miner Metab 19:76–83

49. **Flanagan AM, Stow MD, Williams R** 1995 The effect of interleukin-6 and soluble interleukin-6 receptor protein on the bone resorptive activity of human osteoclasts generated in vitro. J Pathol 176:289–297

50. **Adebanjo OA, Moonga BS, Yamate T, Sun L, Minkin C, Abe E, Zaidi M** 1998 Mode of action of interleukin-6 on mature osteoclasts. Novel interactions with extracellular Ca2+ sensing in the regulation of osteoclastic bone resorption. J Cell Biol 142:1347–1356

51. **Ueland T, Brixen K, Mosekilde L, Mosekilde L, Flyvbjerg A, Bollerslev J** 2003 Age-related changes in cortical bone content of insulin-like growth factor binding protein (IGFBP)-3, IGFBP-5, osteoprotegerin, and calcium in postmenopausal osteoporosis: a cross-sectional study. J Clin Endocrinol Metab 88:1014–1018

52. **O'Brien CA, Gubrij I, Lin SC, Saylors RL, Manolagas SC** 1999 STAT3 activation in stromal/osteoblastic cells is required for induction of the receptor activator of NF-κB ligand and stimulation of osteoclastogenesis by gp130-utilizing cytokines or interleukin-1 but not 1,25-dihydroxyvitamin D3 or parathyroid hormone. J Biol Chem 274:19301–19308

53. **Kim K, Lee J, Kim JH, Jin HM, Zhou B, Lee SY, Kim N** 2007 Protein inhibitor of activated STAT 3 modulates osteoclastogenesis by down-regulation of NFATc1 and osteoclast-associated receptor. J Immunol 178:5588–5594

54. **Zhang Z, Welte T, Troiano N, Maher SE, Fu XY, Bothwell AL** 2005 Osteoporosis with increased osteoclastogenesis in hematopoietic cell-specific STAT3-deficient mice. Biochem Biophys Res Commun 328:800–807

55. **Sims NA, Jenkins BJ, Quinn JM, Nakamura A, Glatt M, Gillespie MT, Ernst M, Martin TJ** 2004 Glycoprotein 130 regulates bone turnover and bone size by distinct downstream signaling pathways. J Clin Invest 113:379–389

56. **Minegishi Y, Saito M, Tsuchiya S, Tsuge I, Takada H, Hara T, Kawamura N, Ariga T, Pasic S, Stojkovic O, Metin A, Karasuyama H** 2007 Dominant-negative mutations in the DNA-binding domain of STAT3 cause hyper-IgE syndrome. Nature 448:1058–1062

57. **Holland SM, DeLeo FR, Elloumi HZ, Hsu AP, Uzel G, Brodsky N, Freeman AF, Demidowich A, Davis J, Turner ML, Anderson VL, Darnell DN, Welch PA, Kuhns DB, Frucht DM, Malech HL, Gallin JI, Kobayashi SD, Whitney AR, Voyich JM, Musser JM, Woellner C, Schaffer AA, Puck JM, Grimbacher B** 2007 STAT3 mutations in the hyper-IgE syndrome. N Engl J Med 357:1608–1619

58. **Grimbacher B, Holland SM, Gallin JI, Greenberg F, Hill SC, Malech HL, Miller JA, O'Connell AC, Puck JM** 1999 Hyper-IgE syndrome with recurrent infections—an autosomal dominant multisystem disorder. N Engl J Med 340:692–702

59. **Liu H, Ma Y, Cole SM, Zander C, Chen KH, Karras J, Pope RM** 2003 Serine phosphorylation of STAT3 is essential for Mcl-1 expression and macrophage survival. Blood 102:344–352

60. **Schuringa JJ, Schepers H, Vellenga E, Kruijer W** 2001 Ser727-dependent transcriptional activation by association of p300 with STAT3 upon IL-6 stimulation. FEBS Lett 495:71–76

61. **Wen Z, Zhong Z, Darnell Jr JE** 1995 Maximal activation of transcription by Stat1 and Stat3 requires both tyrosine and serine phosphorylation. Cell 82:241–250

62. **Ceresa BP, Pessin JE** 1996 Insulin stimulates the serine phosphorylation of the signal transducer and activator of transcription (STAT3) isoform. J Biol Chem 271:12121–12124

63. **Lim CP, Cao X** 1999 Serine phosphorylation and negative regulation of Stat3 by JNK. J Biol Chem 274:31055–31061

64. **Chung J, Uchida E, Grammer TC, Blenis J** 1997 STAT3 serine phosphorylation by ERK-dependent and -independent pathways negatively modulates its tyrosine phosphorylation. Mol Cell Biol 17:6508–6516

65. **Jain N, Zhang T, Fong SL, Lim CP, Cao X** 1998 Repression of Stat3 activity by activation of mitogen-activated protein kinase (MAPK). Oncogene 17:3157–3167

66. **Ng YP, Cheung ZH, Ip NY** 2006 STAT3 as a downstream mediator of Trk signaling and functions. J Biol Chem 281:15636–15644

67. **Yang J, Liao X, Agarwal MK, Barnes L, Auron PE, Stark GR** 2007 Unphosphorylated STAT3 accumulates in response to IL-6 and activates transcription by binding to NFκB. Genes Dev 21:1396–1408

68. **Kwan Tat S, Padrines M, Theoleyre S, Heymann D, Fortun Y** 2004 IL-6, RANKL, TNF-α/IL-1: interrelations in bone resorption pathophysiology. Cytokine Growth Factor Rev 15:49–60